THE ROLE OF SHEAR-FRICTION ON PULL-OUT FRACTURED BASED MODELING OF NYLON 600 WITH CLUMPED FIBER END

Rr. M.I. Retno Susilorini[1]

[1]*Lecturer, Civill Engineering Study Program, Faculty of Engineering, Soegijapranata Catholic University, Jl. Pawiyatan Luhur IV/1, Bendan Dhuwur, Semarang, Telp 024-8441555, email: susilorini@unika.ac.id; retno_susilorini@yahoo.com*

Fiber pull-out modeling is engaged to bond mechanism of the interface between fiber and cementitious matrix. Hereby, the bond interface takes an important role in determining the whole composites structure performance. When a slippery fiber of nylon 600 is applied into "fiber-reinforced cementitious composite" (FRCC), then the bond interface mechanism should be increased to reach a better performance of whole composites. The clumped fiber end condition indicates some performance improvements, rather than the straight one. Advancement of the previous Susilorini's model of fiber pull-out with clumped embedded fiber end will show that shear-friction stress τ takes major contribution in modeling of nylon 600 with clumped fiber end. The pull-out process involved stable fracture and unstable processed that are being specific interest in this research. The research delivers experimental and analytical methods. The experimental method conducts pull-out test with pull-out specimens categorized into specimens with straight fiber end and also specimens with clump fiber end. The fiber is nylon 600 made in Indonesia, diameter of 1.1 mm, and fiber embedded length l_f of 100 mm. A computerized closed-loop universal testing machine is going to be precise equipment measuring the load and displacement of specimens during the pull-out test. The analytical method is modeling the fiber pull-out with clumped fiber end and resulting some formulas and theories for the process of fiber pull-out with clumped fiber end. The experimental results show that specimens with clumped fiber end reach loads about 1200-1400 N that are 14-35% higher that specimens with straight fiber end while the maximum displacement of those specimens reach around 100 mm. The analytical method successfully results the fiber pull-out with clumped fiber end model, and meet a finding of formulas and theories. The model of fiber pull-out with clumped fiber end model fit the experimental results. It is also found that maximum shear-friction stress τ valued as 2.775 MPa with parabolic curve of shear-friction τ and displacement δ relationship. This research meets several theories which are new, specific and significant, they are: (a) The clumped embedded fiber end condition generates parabolic curve of shear-friction stress τ and displacement relationship; (b) shear-friction τ is emerged to against the fiber tension load; (c) The higher bond capacity $\overline{\sigma}_m$ is, the higher shear-friction stress τ will be; (d) The length of stable crack is determined by the position of crack arrester; (e) A new equation derived for load P_n for a model for fiber pull-out of nylon 600 with clumped embedded fiber end which is involves the shear-friction stress τ; and (f) The clumped embedded fiber end improves the pull-out load of nylon 600 fiber pull-out specimens.

Keywords: model, pull-out, nylon 600, shear-friction, clumped fiber end

1. INTRODUCTION

It is known that fiber has been used to be applied in the composites to increase the composite's performance since ancient period. The fiber existence in composites surprisingly shows many advantages of crack delaying and resisting [5]. Hence, fiber

takes an important role in determining whole "fiber-reinforced cementitious composite" (FRCC) performance.

The application of synthetic fiber into FRCC is believed becomes advantage in improving it performance. Nylon fiber is a good example of success effort to reach great tensile ductility of FRCC. One to be noted, nylon fibers is unique as mentioned by [9]. During stretching condition, nylon fiber constricts many times and perform two moving surface waves along the fiber length. This phenomenon is called 'yield point elongation' that has magnitude of 200%-300% of initial fiber length. Later, because of the nylon viscosity, the load may gradually decrease while the fiber length becomes longer two or three times. The multiple constrictions of nylon fiber appeared by 'jagged' phenomenon of stress-strain or load-displacement curves.

Same similar 'jagged' phenomenon happened with mild steel [9], aluminium alloy [9], and nylon [10] and [1]. The application of local (Indonesia) made nylon fiber for concrete has established by previous researches [11], [12], and [1]. The research of [11], [12] used flexural beam and cylinder fiber concrete specimens with straight and clumped short fibers and found that flexural and splitting tensile strength of nylon fiber concrete is higher than the plain concrete. It was also investigated by [11], [12], that wider crack width is found on plain concrete. The research of [1] established pull-out model using pull-out and fracture specimens with straight fibers that established many theories of unstable and stable cracks, the presence of crack arrester, equations for bond capacity $\overline{\sigma}_m$ and Poisson's ration of fiber relation, fiber stress σ_s and matrix stress σ_m relation at the time of failure, stable crack length, load for pull-out and fracture pull-out models, determination of bond capacity by using stable crack, existing of slip stage and strain-hardening stage, and also the possibility of crack arrester presence.

Significant effort in determining the bond mechanism between fiber and cementitious matrix deliver a deep review of fiber pull-out modeling. In FRC, the interface between fiber and matrix behaviour and performance will be predicted by pull out tests. While the tensile ductility performance is a must, the using of synthetic fibers in FRC obviously presents added values, that are strain-hardening property [1], higher tension strength, elastic modulus, and various fiber surfaces [6], high performance as alike steel performance [7], and even higher compressive stress for fiber concrete that its nylon fibers are irradiated by gamma [8].

Fiber pull-out modeling is engaged to bond mechanism of the interface between fiber and cementitious matrix. Hereby, the bond interface takes an important role in determining the whole composites structure performance. When a slippery fiber of nylon 600 is applied into FRCC, then the bond interface mechanism should be increased to reach a better performance of whole composites. The clumped fiber end condition indicates some performance improvements, rather than the straight one.

When a slippery fiber of nylon 600 is applied into "fiber-reinforced cementitious composite" (FRCC), then the bond interface mechanism should be increased to reach a better performance of whole composites. The clumped fiber end condition indicates some performance improvements, rather than the straight one. This paper delivers the advancement of the previous Susilorini's model [3] of fiber pull-out with clumped embedded fiber end by applying shear-friction stress τ into fractured based modeling of nylon 600 with clumped fiber end. The pull-out process involved stable fracture and unstable processed that are being specific interest in this research.

2. METHODS OF RESEARCH

The research delivers experimental and analytical methods. The experimental method conducts pull-out test with pull-out specimens described by Figure 1, categorized into specimens with straight fiber end and also specimens with clump fiber end. The clumped embedded fiber end condition was made by burning the end of fiber until the fiber end change into clumped form. The fiber is nylon 600 made in Indonesia, diameter of 1.1 mm, and fiber embedded length l_f of 100 mm. Mix design for cementitious matrix is defined as ratio of cement : sand : water as 1:1:0.6. A computerized closed-loop universal testing machine is going to be precise equipment measuring the load and displacement of specimens during the pull-out test. The pull-out test set-up is described by Figure 2.

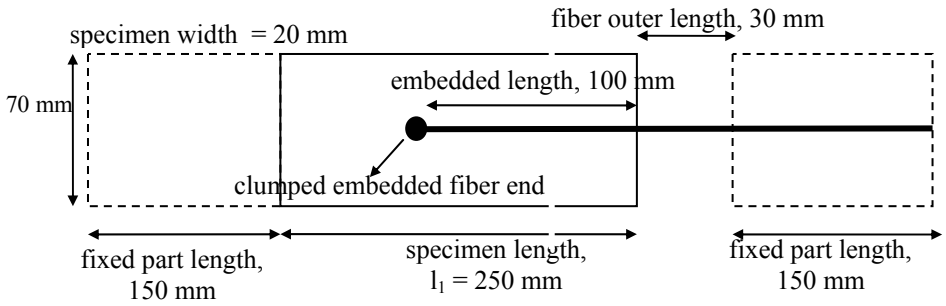

Figure 1. Dimensions of Pull-Out Specimen with Clumped Embedded Fiber End

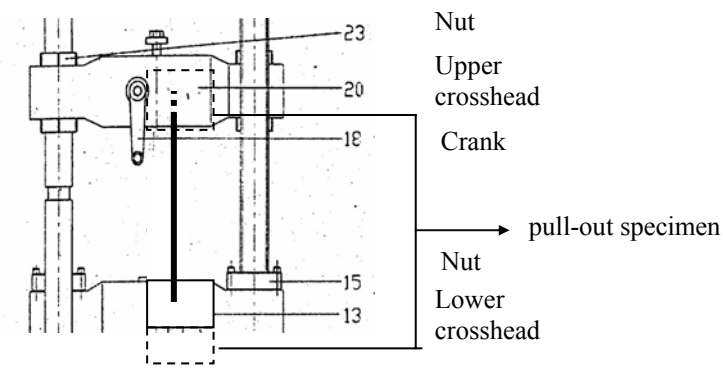

Figure 2. Pull-Out Test Set-Up

The analytical method is modeling the fiber pull-out with clumped fiber end and resulting some formulas and theories for the process of fiber pull-out with clumped fiber end. The phenomenon of stable and unstable fracture is being specific interest and concern in this research. This new model is the advancement of the previous Susilorini's model [3] of fiber pull-out with clumped embedded fiber end that applies shear-friction stress τ into fractured based modeling of nylon 600 with clumped fiber end.

3. RESULTS, MODELING, AND DISCUSSION

3.1. Results

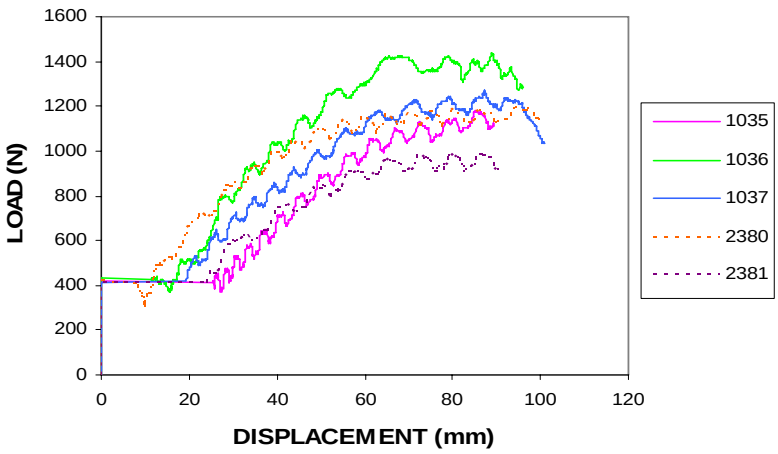

Figure 3. Load-displacement Relation of Pull-Out Test with Straight and Clumped Fiber End

It is found by experimental result that nylon fiber has had average maximum tension stress of 1471.21 MPa, average maximum strain of 0.89, average maximum elongation of 84.11%, and average maximum tension load of 1398.13 N.

Obviously, the 'jagged' phenomenon performs on the relation of load-displacement (P-δ) and stress-strain (σ–ε) curves. For critical Poisson's ratio of fiber of $\bar{\nu} = 0.47$, the critical strain of nylon will reach $\bar{\varepsilon} = 0.29$. The experimental results noted that pull-out specimens with straight and clumped fiber end perform several stages of pull-out process (Figure 3): (a) Pre-slip stage, (b) slip stage, and (c) Strain-hardening stage.

The pull-out test results with straight fiber end found pre-slip loads are about 400-430 N and pre-slip displacements of no more than 0.1 mm. The slip loads have been found in the same range of pre-slip loads with displacements of 3-30 mm. The strain-hardening loads are observed as 900-1200 N as regard. For pull-out test results with clumped fiber end, the pre-slip loads are ranged about 400-430 N with pre-slip displacements of no more than 0.1 mm. The slip loads had the same range of pre-slip loads with displacements of 3-30 mm while strain-hardening loads are about 1200-1400 N and displacement of 20-100 mm. It is also fond that the pre-slip stress are ranged about 400-460 MPa with pre-slip strain of no more than 0.001. The slip stress had the same range of pre-slip loads with strain of 0.001-0.155, while strain-hardening loads are ranged about 1400-1500 MPa and strain of 0.15-0.9.

3.2. Modeling

A first pull-out model has been derived by [1] for straight embedded fiber end that is improved into clumped embedded fiber end [3]. In this research, the model of [3] is refined and improved. In this new model, many aspects are considered: (1) Fracture capacity of embedded fiber is a function of Poisson's ratio of fiber, (2) Some stages exist during the pull-out and fracture pull-out process, (4) A 'jagged' phenomenon

exists on strain-hardening part of load-displacement (P-δ) and stress-strain (σ–ε) curves of pull-out, (4) Unstable and stable fracture process phenomenon exist during the pull-out process, and (5) Shear-friction τ is emerged to against the fiber tension load.

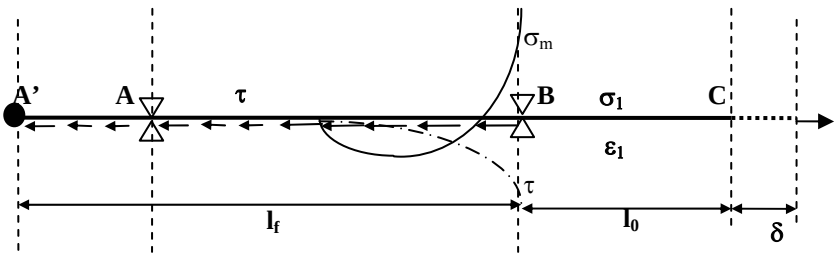

Figure 4. Pull-Out Model with Clumped Embedded Fiber End at Elastic Stage

Figure 4 describes the first principal thought of the model. A piece of embedded fiber (A'A) with clumped embedded fiber end at A' which is constrained at A and B but free at C. Free end fiber length named l_0 and embedded fiber end called l_f. A displacement δ is applied at C and both cementitious matrix and fiber are still in composites condition. The force resistance of clumped fiber end will emerge shear-friction stress τ that is distributed along the fiber-matrix interface. The value of matrix stress σ_m increases until $\sigma_m = \overline{\sigma}_m = \sigma_m(\overline{v})$ which represents bond capacity at the time of crack. It is called the ultimate fracture tension capacity. The strain and stress at BC:

$$\varepsilon_1 = \frac{\delta}{l_0} \tag{1}$$

$$\sigma_1 = \varepsilon_1 E_s \tag{2}$$

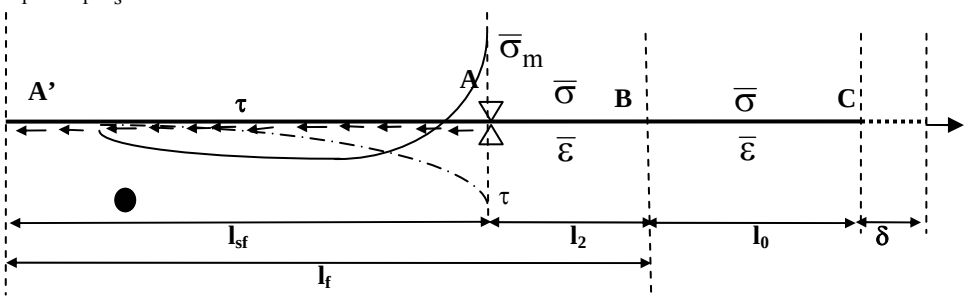

Figure 5. Pull-Out Model with Clumped Embedded Fiber End at Unstable Fracture Process

A crack will be created when the displacement δ keeps growing. This crack performs unstable fracture process. After a crack created, the stress of the composite then being transferred to the fiber. By crack formation, unstable fracture process phenomenon will release the constraint at B (Figure 5). The crack length is growing to be as long as l_2 and constraint at A still can remove to left side. When the crack length l_2 is longer than embedded length l_f, fiber may be pulled-out. The shear-friction stress τ is then distributed along A'A. The length of shear-friction stress τ distribution is called l_{sf}. It should be noted that the higher bond capacity is, the higher shear-friction stress τ will be.

An unstable fracture process may grow into stable fracture process which. Assume that a crack formed as (Figure 6), then the increasing of displacement δ will also increase strain ε_1 and stress σ_1 at B'B. Those strain ε_1 and stress σ_1 increasing will cause the achieving critical value of matrix stress $\overline{\sigma}_m$ and strain $\overline{\varepsilon}$. Therefore, the displacement δ increasing repeated at B' at the same time a new crack of another formed Δx at the left side of fiber. During the crack Δx formation, the shear-friction stress τ gives contribution along the embedded fiber to against the displacement of fiber free-end. It happened continuously until constraint A is fixed. Hence, the constraint A becomes 'crack arrester' that will prevent crack growth. In case, the crack will be stopped to grow and crack length remains l_2. Once stable crack length l_2 achieved, then strain at l_0 part transfer to l_2 part. The stress and strain become:

$$\varepsilon_1 = \varepsilon_{l2} = \varepsilon_0 = \varepsilon_r \tag{3}$$

$$\sigma_1 = \sigma_{12} = \sigma_0 = \sigma_r \tag{4}$$

$$\varepsilon_r = \frac{\delta}{l_0 + l_2} \tag{5}$$

When $\overline{\sigma}_m = \sigma_m(\overline{v})$ is achieved and strain at AC is $\varepsilon = \overline{\varepsilon}$, then $\delta = \overline{\delta}$ and strain:

$$\varepsilon = \overline{\varepsilon} = \frac{\overline{\delta}}{l_0 + l_2} \text{ where } \overline{\varepsilon} = \varepsilon(\overline{v}) \tag{6}$$

The stable crack is formulated as:

$$l_2 = \frac{\overline{\delta} - \overline{\varepsilon} l_0}{\overline{\varepsilon}} \tag{7}$$

The shear-friction stress τ can be formulated as:

$$\tau_f = \frac{\varepsilon E A^2}{A_{fl}} \tag{8}$$

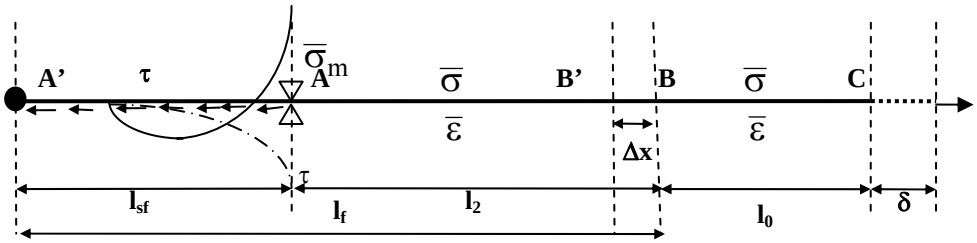

Figure 6. Pull-Out Model with Clumped Embedded Fiber End at Stable Fracture Process

The model represents a P-δ (load-displacement) curve (Figure 7) that consists of 3 (three) stages of pull-out process: (a) Stage of pre-slip, (2) Stage of slip, and (3) Stage of strain-hardening. During the stage of pre-slip, cracks have not been created, so that the fracture process phenomenon not exists. After critical matrix stress $\overline{\sigma}_m$ exceeded, a crack is formed, the stage of slip and unstable fracture process has just begun. The unstable fracture process keeps going and crack length increases until stable crack length l_2 reached at the end of stage of slip. The stable crack length l_2 will be achieved after the unstable fracture process changed to stable fracture process. The stable fracture process is going to be continued by the stage of strain-hardening. In this stage, the increase of the strain ε will increase the stress σ until the fiber is getting broken. It should be noted that clumped embedded fiber end condition emerges shear-friction

stress τ that is distributed along the embedded fiber. Obviously, the shear-friction stress τ will against the fiber tension load and improve the specimen's pull-out load.

.

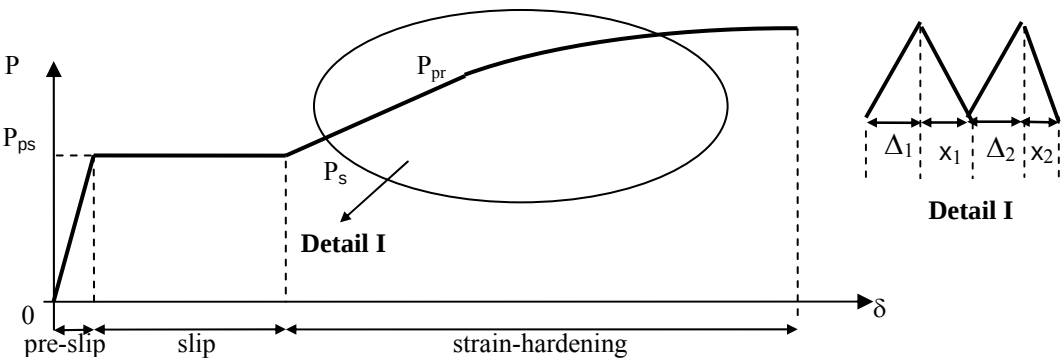

Figure 7. P-δ (load-displacement) Relation of Theoretical Pull-Out Model

Formulation of the theoretical model is defined by equation (9) as follow:

$$P_n = \left(r_{\Delta I}\frac{a_1}{a_2}E_{ps}A\right) + \left(r_{\Delta II}\frac{a_1}{a_2}E_sA\right) + \left(C_1 r_{\Delta III}\frac{a_1}{a_2}E_{pr}A\right) - C_2\tau_f \quad (9)$$

Where:

$$\text{For stage of slip: } \tau_f = \left(\frac{r_{\Delta II}\frac{a_1}{a_2}E_sA^2}{A_{fl}}\right) \quad (10)$$

$$\text{For stage of slip: } \tau_f = \left(\frac{r_{\Delta III}\frac{a_1}{a_2}E_{pr}A^2}{A_{fl}}\right) \quad (11)$$

The constants of $C_1 = 4.645, C_2 = 0.1$ for stage of slip and $C_1 = 1.5, C_2 = 0.25$ for stage of strain hardening. The range value of E_s, E_{ps}, dan $E_{pr} = E_n$ for pull-out model is: $500000 \leq E_{ps} \leq 650000$, $2000000 \leq E_{s\ initial} \leq 650000$, $500 \leq E_{s\ end} \leq 1500$, $400 \leq E_{pr} \leq 2000$. The theoretical model above has compared to experimental results. The P-δ (load-displacement) curves and σ-ε (fiber stress-strain) curve of experimental result and model (Figure 8 and 9) and also the τ_f-ε (shear-friction stress-strain) curve of model (Figure 10).

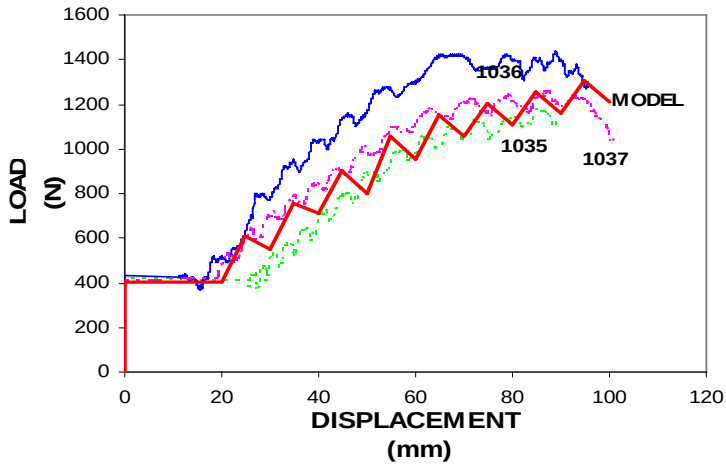

Figure 8. Load-displacement Relation of Experimental Result and Model

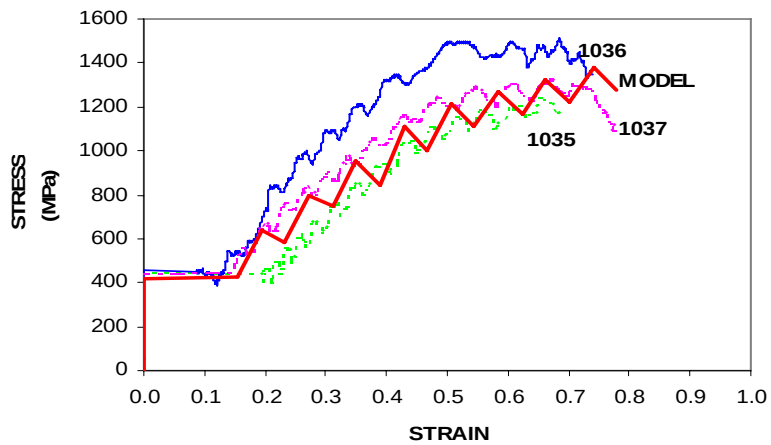

Figure 9. Stress-strain Relation of Experimental Result and Model

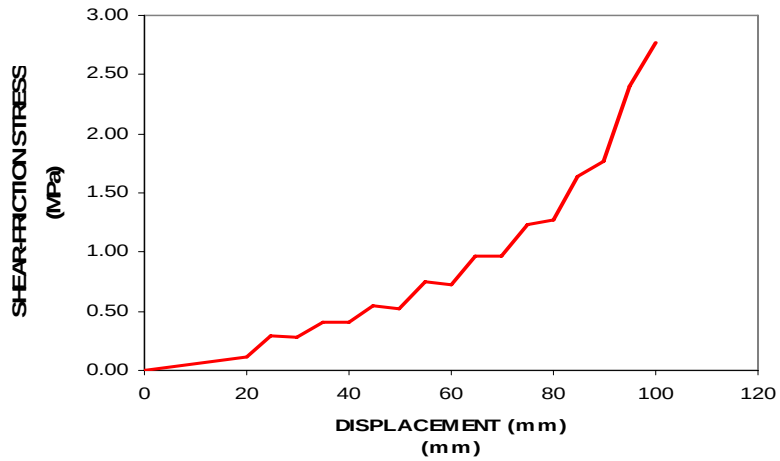

Figure 10. Shear-friction stress-strain Relation of Experimental Result and Model

3.3.Discussion

The research has proved that the 'jagged' phenomenon performs on the relation of load-displacement (P-δ) and stress-strain (σ–ε) curves because of the nylon unique characteristics of constriction and viscosity. This phenomenon cannot be found with any other fiber materials (except mild steel and aluminium alloy). The stages of pull-out process (stage of pre-slip, stage of slip, and stage of strain-hardening) performs strong character of unstable and stable fracture phenomenon.

Figure 8 and 9 show that the model fit to the experimental results. The maximum strain of both model and experimental results (0.8) are lower than maximum strain of nylon fiber tension test (0.89). It is found that the pull-out load of clumped fiber end specimens is 14-35% higher than the pull-out load of straight embedded fiber end specimens (Figure 3). The reason of lower strain and the pull-out load improvement is because of the clumped embedded fiber end condition generates higher shear-friction stress τ to against the fiber tension load will improve the specimen's pull-out load.

It should be noted that the clumped embedded fiber end condition will emerge higher shear-friction stress τ that is distributed along the embedded fiber to against the displacement of fiber free-end. The parabolic curve of shear-friction stress τ and displacement relation emphasizes that the higher bond capacity $\overline{\sigma}_m$ is, the higher shear-friction stress τ will be.

4. CONSLUSIONS

This research meets several theories, which are new, specific and significant, they are:

(a) The clumped embedded fiber end condition generates parabolic curve of shear-friction stress τ and displacement relationship;
(b) shear-friction τ is emerged to against the fiber tension load;
(c) The higher bond capacity $\overline{\sigma}_m$ is, the higher shear-friction stress τ will be;
(d) The length of stable crack is determined by the position of crack arrester;
(e) A new equation derived for load P_n for a model for fiber pull-out of nylon 600 with clumped embedded fiber end which is involves the shear-friction stress τ;
(f) The clumped embedded fiber end improves the pull-out load of nylon 600 fiber pull-out specimens

ACKNOWLEDGMENT:

The authors gratefully acknowledge UBCHEA (United Board of Higher Christian Education) for supporting the research grant (2005-2007), Prof. Ir. Moh. Sahari Besari, MSc., PhD., and Prof. Bambang Suryoatmono, PhD., for their great contributions of ideas, discussions, and intensive assistance.

NOTATION

A fiber section area (mm^2)
A_{fl} fiber surface area (mm^2)
A_m matrix surface area (mm^2)
C_1 constant 1
C_2 contant 2

D fiber diameter (mm)
E_{pr} modulus of elasticity at stage of strain-hardening (MPa)
E_{ps} modulus of elasticity at stage of pre-slip (MPa)
E_s modulus of elasticity at stage of slip (MPa)
P, P_n tension load (N)
a_1 total displacement of a stage (mm)
a_2 initial length of specimen or fiber that is specific for every stage (mm)
b specimen width (mm)
$r_{\Delta I}$ ratio of total free-end fiber displacement of free-end at stage of pre-slip
$r_{\Delta II}$ ratio of total free-end fiber displacement of free-end at stage of slip
$r_{\Delta III}$ ratio of total free-end fiber displacement of free-end at stage of strain-hardening
l_0 initial outer fiber length (mm)
l_2 stable crack length (mm)
l_f embedded fiber length (mm)
l_{sf} length of shear-friction (mm)
x_i relaxation length for n at stage of strain-hardening (mm)
Δ_i free-end displacement for n at stage of strain-hardening (mm)
σ_1 fiber stress at the midldle of right side of matrix (MPa)
σ_{l2} fiber stress at l_2 part when stable crack length achieved (MPa)

REFERENCES:

1. Susilorini, Retno, M.I. (2007) *Model Masalah Cabut-Serat Nylon 600 Tertanam dalam Matriks Sementitis yang Mengalami Fraktur*, Unpublished PhD Dissertation, Postgraduate Program, Parahyangan Catholic University, Bandung.

2. Susilorini, Retno, Rr. M.I. (2007) Fractured Based Approach for Structural Element Design – Safe Building, Safe City, *In: Third International Conference on Economic and Urban Management "City Marketing, Heritage, and Identity"*, 24-25 August, PMLP Unika Soegijapranata, Semarang, 451-465.

3. Susilorini, Retno, Rr. M.I. (2007) The Performance Improvement of Fiber Pull-Out of Nylon 600 with Clumped Fiber End, *In: First International Conference of European Asian Civil Engineering Forum (EACEF)*, 26-27 September, Pelita Harapan University, Lippo Karawaci, Jakarta, D64-D71.

4. Susilorini, Retno, Rr. M.I. (2007) Integral-J Kritis untuk Model Elemen Hingga pada Cabut Serat Fraktur Nylon 600, *In: Tiga Roda Forum "Perkembangan Terkini Teknologi dan Rekayasa Konstruksi Beton di Indonesia"*, 12 December, Hotel Bumi Karsa - Bidakara, Jakarta, 1-14.

5. Naaman, AE., Namur, GG., Alwan, JM., Najm, HS. (1990) Fiber Pullout and Bond Slip. I: Analytical Study. *Journal of Structural Engineering, ASCE*, **117**(9), 2769-2790.

6. Li, V.C., Chan, Y.W., Wu, H.C. (1994) Interface Strengthening Mechanism in Polymeric Fiber Reinforced Cementitious Composites, *In: Proceedings of International Symposium on Brittle Matrix Composites* (eds. Brandt, A.M, Li, V.C., Marshall, L.H), IKE and Woodhead Publ, Warsaw, 7-16.

7. Clements, M. (2002) Synthetic as Concrete Reinforcement, *In: Concrete Magazine*, United Kingdom, September, 37-38.

8. Martinez-Barrera, G (2006) Concrete Reinforce with Irradiated Nylon Fibers. *Journal of Material Research*, **21**(2), February, 484-491.

9. Nadai, A. (1950) *Theory of Flow and Fracture of Solids*. Volume I, McGraw-Hill Company. Inc, New York, USA.

10. Avarett, RD (2004) *Fracture Mechanics of High Performance Nylon Fibers*, Thesis, Georgia Institute of Technology, USA.

11. Suseno, W., Saptono, K., Yosephine, P., Andre, S. (2000) Pengaruh Fiber Senar Pancing Terhadap Kuat Lentur Beton. *Jurnal Sipil Supra*, **2**(4), April-June, 116-124.

12. Suseno, W., Saptono, K., Sapthina, M., Wibowo, M. (2000) Uji Tarik Belah pada Beton Serat dengan Senar Pancing, *Jurnal Sipil Supra*, **2**(6), Oktober-Desember, 238-247.